

Ultrafast solid-phase chemical synthesis of BaTiO₃ initiated by millimeter-wave radiation

© S.V. Sintsov, N.V. Chekmarev, K.I. Rybakov, A.A. Sorokin, E.I. Preobrazhensky, A.V. Vodopyanov

Federal Research Center A.V. Gaponov-Grekhov Institute of Applied Physics of the Russian Academy of Sciences,
603950 Nizhny Novgorod, Russia
e-mail: sins@ipfran.ru

Received September 22, 2025

Revised November 6, 2025

Accepted November 27, 2025

This paper presents the results of a study of the solid-phase synthesis of barium titanate using continuous microwave radiation from a 24 GHz process gyrotron in a multimode reactor. It is demonstrated that in localized regions of small-scale superheated instabilities initiated by millimeter-wave radiation in the initial stoichiometric reaction mixture of ultrafine barium carbonate and titanium dioxide powders of bulk density, the synthesis process can proceed in 5–7 minutes, ensuring a target product yield of 90%. A realistic numerical model of a multimode reactor developed, based on an iterative solution of Maxwell's steady-state equations and thermal conductivity, shows that the specific energy input in the regions of small-scale superheated instabilities can reach 670 W/cm³ with an input power of 400 W.

Keywords: barium titanate, chemical synthesis, gyrotron, computer modeling.

DOI: 10.61011/TP.2026.04.63269.273-25

Introduction

High-temperature solid-phase chemical synthesis is one of key processes of obtaining a wide spectrum of functional inorganic materials [1]. The methods based on convection heating of reaction mixtures are characterized by significant inertness, high energy consumption and long synthesis times that are often counted to be many hours. These factors not only increase production costs, but can also result in reduction in quality due to intense grain growth and formation of impurity phases under long high-temperature impact [2,3]. Duration of the solid-phase physical-chemical processes significantly decreases when transiting to heating in a microwave electromagnetic field [4–6]. The main advantage is a mechanism of volume impact, when energy of the electromagnetic field is directly absorbed by a material to be transformed into heat. This approach can provide extremely high heating rates, significantly reduce total energy consumption as compared to convection methods and in some cases it makes it possible to attain target phases at the lower temperatures. Potentially, it can also result in producing products with improved characteristics, for example, with the smaller grain size or the higher phase purity [4–14]. But serious challenges are encountered when practically implementing and industrially scaling these advantages for the solid-phase processes in common microwave systems that operate on magnetrons with a radiation frequency of 2.45 GHz. A fundamental limitation is related to inhomogeneous distribution of the heating electromagnetic field in powder media. Taking into variation of electrodynamic and thermodynamic parameters of the reaction mixture in a dependence on the temperature, it can result in origination of uncontrolled local superheats

(„hot points“), thus impairing synthesis homogeneity and complicating both process control and its scaling.

The present study considers a new approach to microwave solid-phase synthesis, which is based on purposeful initiation and use of small-scale superheated instabilities. Its essence is to use shorter (millimeter) electromagnetic radiation for creating highly-contrast temperature fields, i.e. highly-localized regions of extreme superheating, in the reaction mixture. At the same time, it is possible to create conditions, in which these regions are isolated from a major bulk of the material due to low thermal conductivity of the medium, which is achieved in the reaction mixture of dispersed powders that have a bulk density. A sharp temperature gradient that originates at boundaries of such small-scale superheated instabilities makes it possible to spatially separate a reacted product (in a high-temperature zone) and an unreacted initial substance, thereby providing a high rate and selectivity of the reaction without superheating the entire volume. The present study experimentally demonstrates this mechanism by an example of a reaction of solid-phase synthesis of barium titanate (BaTiO₃) when heating the initial stoichiometric reaction mixture of dispersed powders of barium carbonate (BaCO₃) and titanium dioxide (TiO₂) with continuous millimeter radiation with a frequency of 24 GHz. On the one hand, highly-dielectric properties of barium titanate in combination with a low wavelength of the millimeter radiation create condition for heavy localization of energy release, which is required for controlling the superheated instabilities. On the other hand, this process is selected due to a practical value of this ferroelectric material in modern microelectronics. In order to study a spatial distribution of the temperature in the medium with developed small-scale

superheated instabilities, a realistic numerical model of a multi-mode microwave reactor used in the experiment has been designed.

1. Experimental setup

Fig. 1 shows the diagram and the photo of the multi-mode microwave reactor, which is a close electrodynamic structure that is connected to the round waveguide path of the technological gyrotron with the radiation frequency of 24 GHz and output power of up to 5 kW in a continuous regime [15–17]. A window for inputting microwave radiation is a round quartz wafer of an anti-reflective thickness, which is embedded into a frame of the waveguide path. It functions to protect a source when a gas discharge occurs in the reactor and it propagates towards microwave radiation. An important element of the unit, which electro-dynamically limits the reactor volume, is the filter, which is a tapering section of the round waveguide and designed to prevent propagation of microwave radiation back to the source. Additional reduction of reflection is facilitated by orientation of an output slot of the filter perpendicular to a polarization plane of an excited mode. The reactor zone is designed of two vacuum fitting tees with the flange ports of the CF40 standard. In a described configuration, free ports were used for installation of assemblies for inputting/outputting purging air as well as for visually controlling a process of heating and temperature measurement by means of a two-color infrared pyrometer via a metal-mesh window. The reaction mixture was loaded and unloaded via a quick-

releasing flange port that is designed as two interconnected adapters CF 40–KF 40.

The present study has used the following reagents: barium carbonate (BaCO_3 , a „analytical reagent“ grade, GOST 4158-80, produced by LLC „Vekton“, Russia) with the particle size 1.5–2.0 μm and titanium dioxide (TiO_2 , a „pure“ grade, TU 301-10-020-90, produced by LLC „Krymskii Titan“, Russian) in an anatase modification with the particle size 0.1–0.3 μm . The reaction medium is a stoichiometric mixture of these powders, which is prepared by manually mixing the components for 10 min. The unrammed powder mixture was placed on the aluminum H-beam substrate with the sizes 24 × 50 mm in the form of a thin layer of the thickness 3–4 mm. After weighing, it was placed in the reactor volume for further heating by microwave radiation.

2. Description of the model of the reaction medium

The process of solid-phase chemical synthesis during millimeter wave heating can be described within the a mathematical model that includes self-consistent electrodynamic and thermal problems based on the Maxwell equations and a thermal conductivity equation, respectively. The distribution of the electromagnetic field in the volume of the used reactor is calculated within the electrodynamic problem. The obtained distribution of intensity of the field in the sample being heated is used for calculating a power density of heat sources included in the thermal conductivity equation.

To perform the calculations, it is essential to correctly specify the electrodynamic and thermal-physical properties of the substances involved in the synthesis reaction. The used materials that are dispersed powders at all the stages can be described as multi-phase systems that contain one or several various solid phases and a gas phase that corresponds to space between the powder particles. In case when a typical scale of a system microstructure heterogeneity is much smaller than a length of the electromagnetic wave in a substance, interaction of the electromagnetic field with such materials is described by applying methods based on introduction of averaged characteristics of the medium. Since in the processes considered herein a ratio between volume phase portions can change during the process within wide limits, the averaged properties of the materials are conveniently described in an effective medium approximation [18], which assumes that spherical inclusions of each phase are placed in the medium with sought-after properties. For complex permittivity of the powder medium, this approach results in the equation

$$\sum_i C_i \frac{\varepsilon_i - \varepsilon_{\text{eff}}}{2\varepsilon_{\text{eff}} + \varepsilon_i} = 0, \quad (1)$$

where ε_i — complex permittivity of the i -the component of the mixture (including a void), C_i — the relative volume portion of the i -th component. This algebraic

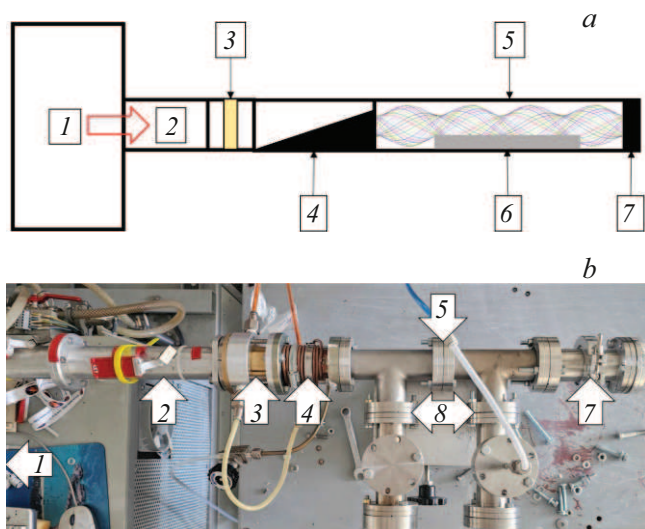
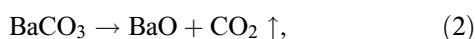


Figure 1. Diagram (a) and the photo (b) of the multi-mode microwave reactor: 1 — the technological gyrotron with the radiation frequency of 24 GHz; 2 — the round waveguide path with the diameter of 32.6 mm; 3 — the anti-reflective quartz window; 4 — the microwave filter; 5 — the multi-mode microwave reactor; 6 — the reaction powder mixture on an H-beam aluminum substrate; 7 — the quick-release flange port for loading/unloading of the powder; 8 — the functional flange ports.

equation, whose power is equal to a number of the various components of the mixture, can be solved in relation to sought-after effective permittivity ϵ_{eff} . The similar equation defines an effective thermal conductivity coefficient of the powder medium λ_{eff} .

An equimolar mixture of bulk powders BaCO₃ + TiO₂ was used as initial substances for the synthesis process in the present study. It was assumed during modeling that the process takes places in two stages: first, BaCO₃ is decomposed at the temperature of 800 K:



and then at the temperature of 1073 K BaTiO₃ is synthesized:



Selection of the temperature of 800 K as a threshold value for the start of a reaction of decomposition of barium carbonate in the model is based on a fact that is given in the literature and says that the temperature of the reaction in the BaCO₃–TiO₂ system has a much lower value as compared to the temperature of thermal decomposition of individual barium carbonate. A pure substance of BaCO₃ demonstrates the start of decomposition at the temperatures above 1700 K, while in the reaction mixture with TiO₂ formation of the barium titanate starts at considerably lower temperatures. The study [19] uses X-ray diffraction analysis to demonstrate that under conditions of microwave heating formation of a crystalline phase of BaTiO₃ is already noticeable at 1073 K, thereby indicating that the reaction of decomposition of carbonate in the mixture takes place at the smaller temperatures. Thus, the initial system is a three-phase one (BaCO₃, TiO₂ and air in pores); besides, an intermediate system for which the calculations were within the temperature interval 800–1073 K (BaO, TiO₂ and air in pores) is a three-phase one as well, while the final system is a two-phase one (BaTiO₃ and air).

Data on the volume portions of the mixture components were calculated based on measurements of the density of the bulk powder. Data on a volume portion (a relative density) of compacted BaTiO₃ were taken from experiments of its microwave sintering at the various temperatures [20].

Data on temperature-dependent high-frequency dielectric properties of various substances are often quite scarce in the literature. Data on permittivity of BaCO₃ were taken from the study [21], so were those on a real part of high-frequency permittivity of TiO₂ from the study [22], and data on high-frequency dielectric losses of TiO₂ were taken from the study [23]. Data on high-frequency permittivity and dielectric losses of BaO were taken from the study [24]. For BaTiO₃, temperature-dependent data on high-frequency permittivity and dielectric losses from the study [25] were used and they were obtained in the processes of microwave heating of a loosely-poured powder and took into account variation of the density during sintering. Where necessary, extrapolation of available dependences into a higher-frequency range was used.

Instead of data on the thermal conductivity coefficient of BaCO₃, temperature-dependent data for CaCO₃ from the study [26] were used. Possible deviations of results, which are related to this replacement, are not too considerable, since they can affect calculation of the temperature field only at the initial stage of heating. Data on the thermal conductivity coefficients of BaO and TiO₂ in a dependence on the temperature were taken from the study [22]. For BaTiO₃, we have used data from the study [27], which are extrapolated into the high-temperature range with taking into account variation of the relative density during sintering. Temperature-dependent data on the thermal conductivity coefficient of air were taken from the study [25].

Specific heat capacity of the mixtures was calculated in an additive method with taking into account molar ratios between the components of the mixture. Data on values of specific heat capacity of the components depending on the temperature were taken from the study [22,28].

A shape of the obtained temperature dependences of the effective parameters of the powder media, which are used during modeling, is shown in Fig. 2.

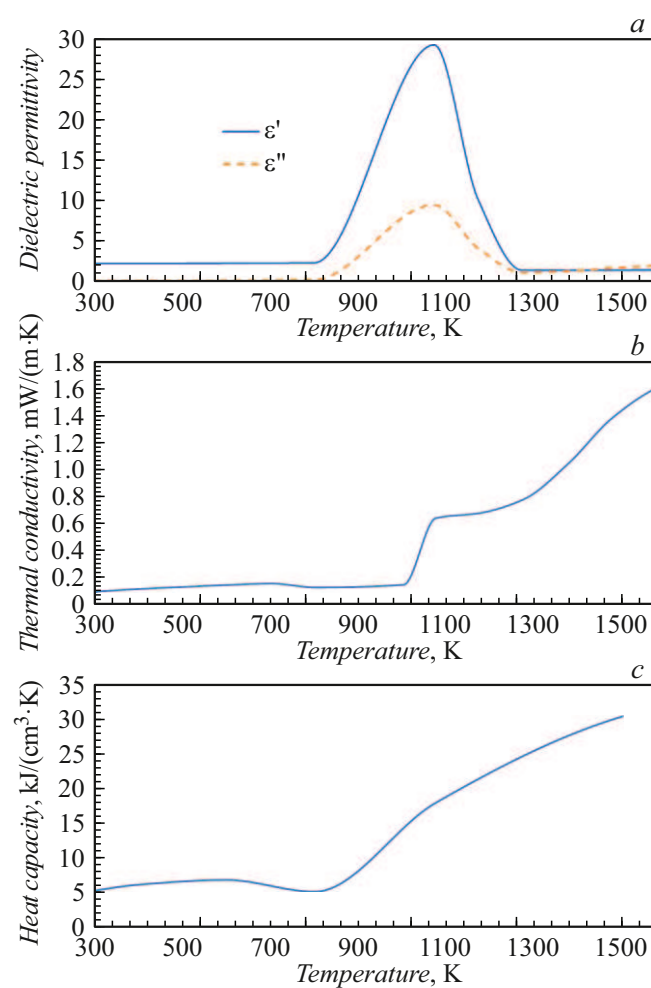


Figure 2. Temperature dependences of the effective parameters of the powder media, which are used during modeling: *a* — complex permittivity, *b* — the thermal conductivity coefficient; *c* — specific heat capacity per a unit volume.

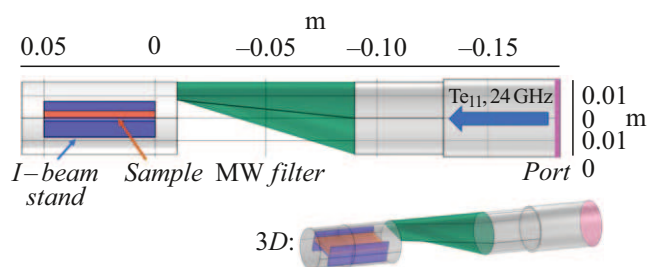


Figure 3. Realistic three-dimensional finite element model of the multi-mode microwave reactor.

3. Numerical modeling

In order to study mechanisms of formation of the small-scale superheated instabilities when heating the powder reaction mixture by electromagnetic radiation of the wavelength millimeter range, we have designed a realistic three-dimensional finite-element model of the microwave multi-mode reactor (Fig. 3) used in the experiments. In addition to the main structural elements, the model includes the round waveguide port at the right boundary, which is excited by the mode TE_{11} with the frequency of 24 GHz and linear polarization.

The self-consistent problem that combines the calculation of propagation and absorption of electromagnetic radiation with modeling of heat transfer was solved by means of an iteration procedure of calculation of the power density of the heat sources included in the thermal conductivity equations and the distribution of the temperature in the medium, which is caused by them. External boundaries of the calculated volume and surface of the metal substrate have an impedance boundary condition specified by the equation (4):

$$\mathbf{n}(\mathbf{E} - Z_s \cdot (\mathbf{n} \times \mathbf{H})) = 0, \quad (4)$$

where Z_s — surface impedance of the material, \mathbf{n} — a unit vector of the normal to the material surface, \mathbf{E} and \mathbf{H} — strengths of the electric and the magnetic field of the wave, respectively. This condition makes it possible to adequately take into account absorption of energy in a

thin skin layer of the metal elements without the need for its detailed resolution in a grid. Radiation reflected from the reactor is absorbed at the input port boundary, where its mode composition is also analyzed for determining the reflection coefficients (S -parameters).

Heat transfer is modeled jointly in the volume of the powder sample and the aluminum H-beam substrate. The heat sources include volume Joule losses calculated based on a distribution of absorbed microwave power in the dielectric sample as well as losses in metal walls of the reactor due to the skin effect. The external boundaries of the sample and the substrate have combined conditions of radiative heat exchange and free convection into the environment specified and these model removal of heat from the system.

Results of modeling for input power of 400 W demonstrate the following key specific features. The distribution of strength of the electric field (Fig. 4) demonstrates a quasi-periodic standing wave structure above the sample. A position of maximums of strength of the electric field directly corresponds to zones of maximum absorption of microwave energy and, therefore, the most intense heat release. Power balance demonstrated a qualitative compliance with the experiment: of 400 W of input power 303 W is absorbed in the very powder sample, 3 W is lost in the walls and 94 W is reflected back.

The distributions of the temperature (Fig. 5, a) and the absorbed power density (Fig. 5, b) have been analyzed to identify their strong spatial correlation. Pronounced localized regions, whose temperature is enough for the solid-phase processes, are formed on the sample surface. These high-temperature zones ($T > 1300$ K) with value-different specific energy deposition are quasi-periodically arranged with a typical distance between the adjacent maximums, which is about 7 mm, which is close to a half of the radiation wavelength in free space ($\lambda = 12.5$ mm). Depending on the value of the specific energy deposition, the typical size of the high-temperature regions varies within 3–8 mm. Movement of the sample does not change qualitatively a pattern of distribution of strength of electric field within the reactor volume, while the regions of formation of superheated instabilities are shifted in relation to the sample. According to results of the calculations,

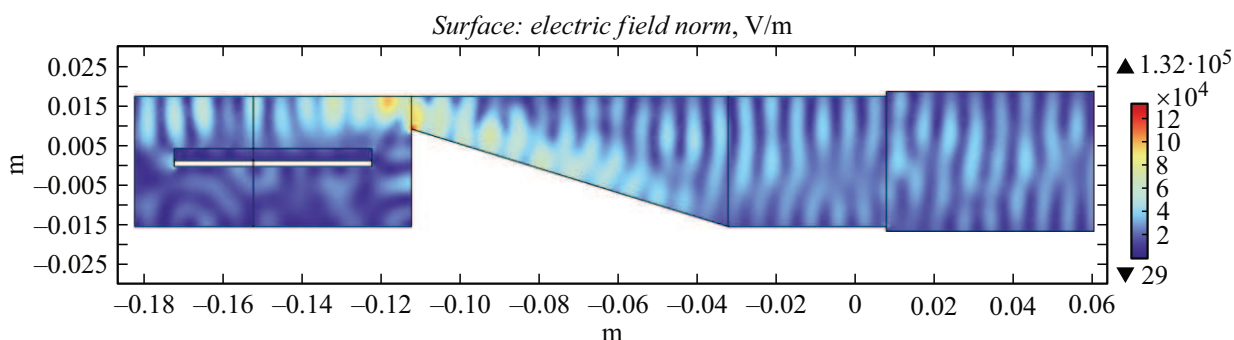


Figure 4. Distribution of strength of the electric field in the model of the multi-mode microwave reactor.

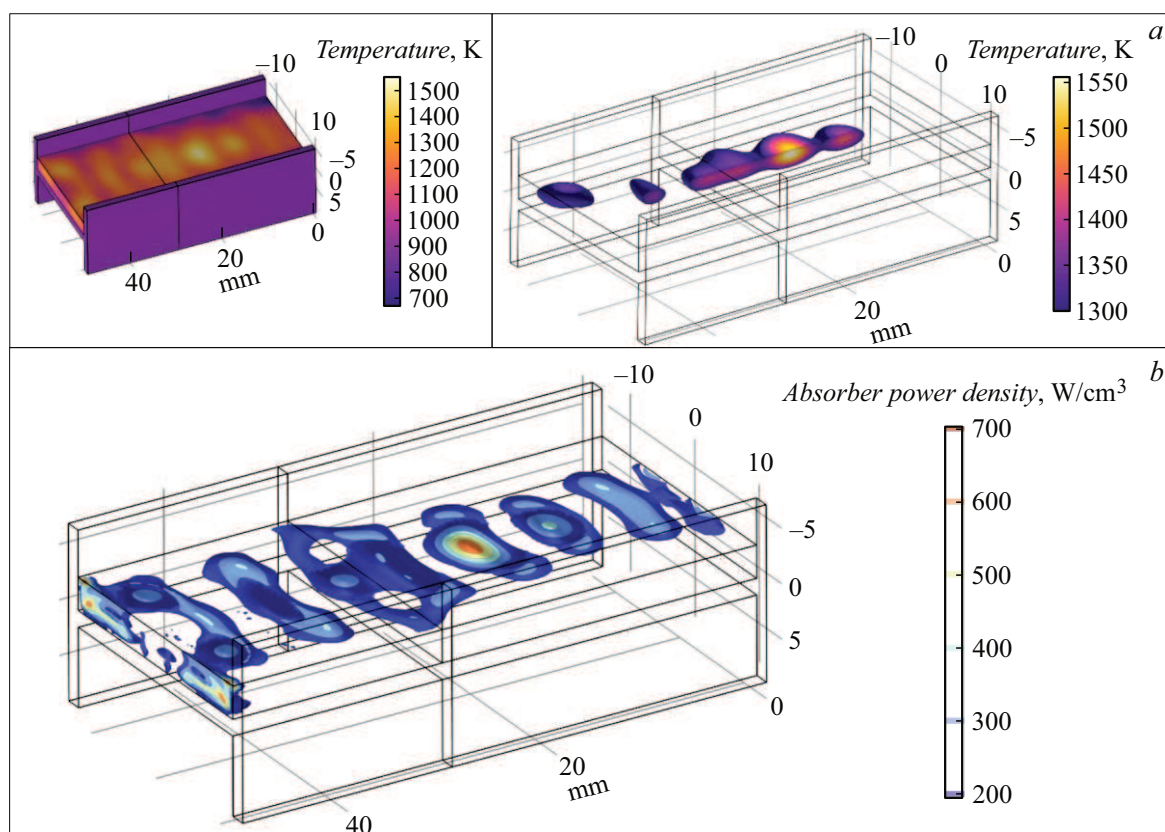


Figure 5. Distribution of the temperature (*a*) and the power density (*b*) in the sample placed in the multi-mode microwave reactor. Input power is 400 W.

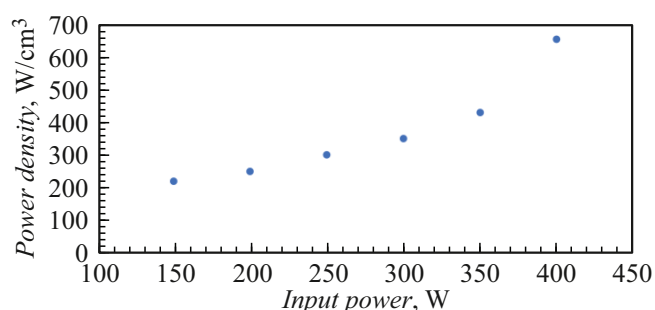


Figure 6. Dependence of the maximum volume density of microwave power in the region with a developed superheated instability on the value of input power.

the maximum specific energy deposition can be up to 670 W/cm³ at the input power of 400 W. At the boundary of the high-temperature regions, a typical temperature gradient is 60 K/mm.

With an increase of input power, the maximum specific energy deposition in the regions with the developed superheated instability increases non-linearly (Fig. 6). Along with it, the typical size of superheated instabilities is also increased up to a state, when adjacent high-temperature regions merge to form a single layer of a target reaction product. For all the tested regimes with various val-

ues of input microwave power, the maximum achievable temperature exceeds 1300 K, thereby meaning a transition through specific features of the temperature dependences of permittivity of the medium, which is specified in the model (Fig. 2, *a*). With the higher input power, the temperature around the maximum energy deposition exceeds 1500 K, which corresponds to melting of barium titanate and is not described within the model of the characteristics of the medium.

4. Experimental part

The process of the solid-phase synthesis was started from inputting microwave radiation, whose power in the experiments done was varied within 200–400 W. In 30–80 s, the surface of the powder layer exhibited red luminescence spots, thereby indicating development of superheated instabilities in these regions. Duration of the process was 1.5–7 min. During heating in the region of origination of the red spots the surface temperature was 600°C–800°C depending on heating power and did not change during the entire process.

The processes done resulted in formation of agglomerated structures under the surface of the powder layer, which have sizes of about 3–6 mm and are located in the

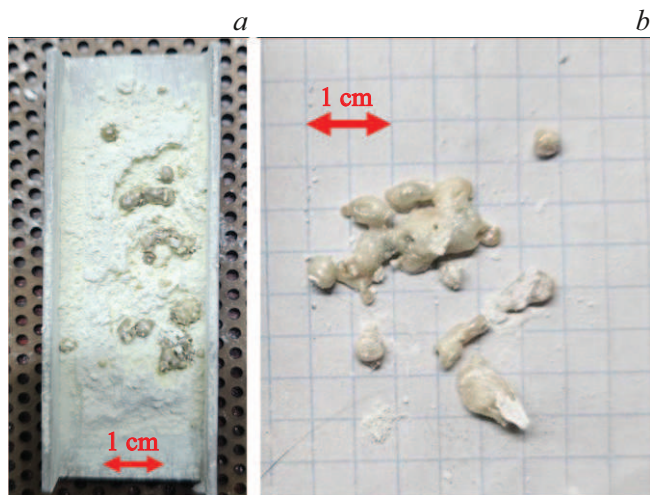


Figure 7. Photos of the powder layer on the aluminum H-beam substrate (a) and agglomerates (b) extracted therefrom, after heating in the multi-mode microwave reactor. The input power is 400 W, the heating time is 7 min.

regions of origination of the red spots during heating. An increase of power and the heating time results in merging of these structures and formation of larger agglomerates. Fig. 7 shows typical photos of the powder layer and the agglomerates extracted therefrom, after heating in the multi-mode microwave reactor. Weighing the sample and the agglomerates extracted therefrom made it possible to estimate a weight loss, which was 13%–15% (mass percent are given hereinafter). It is caused by loss of carbon dioxide during decomposition of barium carbonate and indirectly indicates reaching of the temperature that is enough for occurring of the solid-phase reaction of synthesis of barium titanate.

The produced agglomerates were mechanically ground for X-ray diffraction analysis in an Ultima IV diffractometer (Rigaku, Japan) designed to use $\text{CuK}\alpha$ line emission. Phase identification and quantitative analysis were performed by a Rietveld method using the PDXL 2.0 software and the ICDD database. For an internal standard, corundum ($\alpha\text{-Al}_2\text{O}_3$) was used and it was added to the samples in the amount of 20 wt%. An error of determining the weight portion of the crystalline phases did not exceed $\pm 3\%$. Fig. 8 shows a typical X-ray pattern of ground agglomerates synthesized in the multi-mode microwave reactor.

Detailed analysis identified a significant dependence of the phase composition on the treatment regimes. With power of microwave radiation 200–300 W and the synthesis time 1.5–4 min, a complex multi-component composition was formed to have various polymorphous modifications of BaTiO_3 prevailed. Presence of a monoclinic phase of $\text{BaO}(\text{TiO}_2)_2$ in the amount 6%–7% seems to indicate local barium insufficiency due to kinetic limitations of diffusion under conditions of superfast synthesis. With increasing the power to 300–400 W and the treatment time to 5–7 min,

the phase composition was significantly changed. In these conditions, a tetragonal modification of BaTiO_3 (up to 68%–72%) was dominant, thereby indicating that the reaction occurs more fully and it approaches a thermodynamically equilibrium state. Presence of the hexagonal phase (18%–23%) that is stable at the temperatures above 1430 °C indicates local superheating of reaction zones to the temperatures that significantly exceed a sample-average one. At the maximum heating power, it also exhibited formation of a small amount (up to 3% when duration of the process is 5 min) of nonstoichiometric compounds of the type Ba_2TiO_4 and $\text{Ba}_2\text{Ti}_9\text{O}_{20}$, which are characterized by shortage of barium and oxygen in relation to titanium. Residual amounts of barium carbonate, which are observed in some cases (up to 5%–7%), can be related to specific features of decarbonization under the conditions of superfast synthesis.

The synthesized samples were microstructurally analyzed using the JEOL JSM-6700F scanning electron microscope. 3–5 SEM images were obtained for each sample at various magnifications, thereby making it possible to visually analyze the microstructure. The synthesized samples predominantly exhibited formation of dense sintered particle agglomerates of the size 0.5–8 μm without signs of an anomalous grain growth or formation of elongated porous structures. At the same time, no sign of nanoscale regions of coherent scattering or amorphous phases in all the samples indicates full crystallization of the synthesis products even under the conditions of superfast synthesis.

It is interesting to consider a spatial compliance between the experimentally observed sizes of the agglomerates (3–6 mm) and calculated sizes of the zones of superheated instabilities, which are obtained during numerical modeling. This compliance not only confirms adequacy of the designed numerical model, but also indicates a deterministic nature of the process of formation of superheated instabilities. It was demonstrated by X-ray diffraction analysis that exactly these zones demonstrated the most fully progressing synthesis reactions with formation of the target phases. A typical

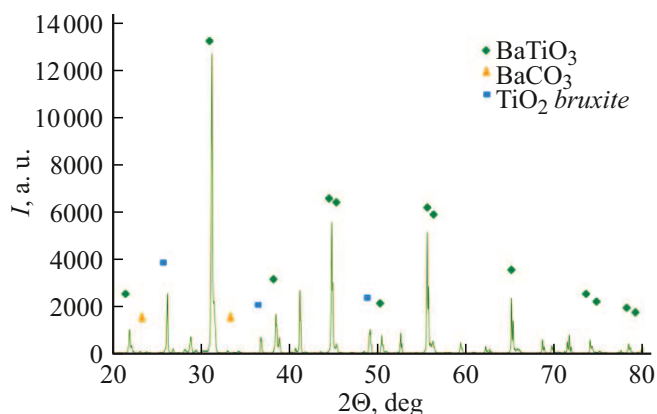


Figure 8. Typical X-ray patterns of ground agglomerates synthesized in the multi-mode microwave reactor. The synthesis regime: 400 W, 7 min.

temperature gradient at boundaries of instability zones, which is at the level of 60 K/mm, creates conditions for spatially separating regions of the reaction and the initial reagents, thereby providing high selectivity of the process.

5. Discussion of results

The experimental and calculated data obtained demonstrate a fundamental difference of the proposed approach from traditional methods of microwave synthesis. While most studies in the field of microwave treatment of materials are directed at suppressing heterogeneities of the temperature field [4,6,12], the present study proposes a paradigm of purposefully creating and using controlled small-scale superheated instabilities. It was possible due to using millimeter radiation, thereby providing heavy space and energy localization of the superheating zones.

A key advantage of the method is achievement of extremely high heating rates in the localized regions while preserving the bulk of the material at the significantly lower temperatures. It creates conditions when kinetics of the solid-state reaction is determined not by classical equations of diffusion balance (which belong to Yander, Ginstling-Brownstein), but processes that are initiated under conditions of the sharp temperature gradients (up to 60 K/mm). The obtained values of specific energy deposition (up to 670 W/cm³) are by an order higher than typical values for the traditional microwave system at 2.45 GHz [6,12], where a typical power density does not exceed 50–100 W/cm³ even in the „hot spots“. It makes it possible to achieve reduction of the synthesis time to several minutes, while it is almost by an order higher in studies on microwave synthesis of barium titanate at the frequency of 2.45 GHz [6].

X-ray diffraction analysis demonstrated formation of highly crystalline barium titanate with a content of the basic phase 88%–96%, which is comparable to the best literature data for the traditional synthesis methods [4]. However, unlike the convection methods that result in formation of large-crystal aggregates [2,3] and classical microwave heating that often causes a nonuniform grain growth [12], the described method provides formation of localized agglomerates of the size 3–6 μm without signs of the anomalous grain growth. This microstructure is explained by short duration of thermal impact and presence of sharp temperature gradients that prevent particle coalescence processes.

It should be noted that the designed approach has certain limitations that are related to temperature stability of the materials being synthesized. When the power exceeds 700 W, melting of barium titanate ($T > 1500$ K) is observed, which requires further improvement of scaled models of the described method. One of the scaled approaches can be use of systems of quasi-optical transformation of millimeter radiation beams, which will make it possible to jointly vary the power density of microwave radiation and the size of

the reaction zone when moving it along a beam focusing line.

Prospects of the designed approach are related to controllability of not only kinetics of the chemical reactions, but also the microstructure of the produced materials by varying radiation parameters. The further development of the method may include use of controlled microwave phase shifters in order to create specified spatial distributions of the temperature field, thereby making it possible to implement principles of additive production in microwave synthesis of functional materials.

Conclusion

The studies have been performed to result in designing of the new approach to microwave solid-phase synthesis, which is based on purposeful initiation and use of small-scale superheated instabilities. It is experimentally demonstrated that a degree of conversion of the initial reagents into the target product in the regions with developed superheated instability is high (more than 90%). Based on the realistic numerical model of the multi-mode microwave reactor, we have obtained values of specific energy deposition in the localized regions of instability development and the temperature gradient achieved at their boundaries. It is demonstrated that varying the parameters of UHV heating makes it possible to purposefully control the phase composition of the product being produced. At the optimal treatment regimes, there is predominant formation of the tetragonal modification of BaTiO₃ (up to 70%–75%), which is of the highest practical interest for ferroelectric applications. Microstructure analysis confirmed formation of fine-disperse agglomerates of the size 0.5–8 μm without signs of the anomalous grain growth, which is caused by suppression of the coalescence processes due to short duration of thermal impact and presence of the sharp temperature gradients at the boundary of the reaction zone. Implementation of the potential of the designed method for creating energy-efficient and high-rate technologies of the solid-phase chemical synthesis requires further investigation of kinetics of the reactions under conditions of extremely fast local heating and optimization of the reactor microwave systems.

Acknowledgments

The solid-phase chemical synthesis during microwave heating was studied with the financial support of Foundation for Assistance to Small Innovative Enterprises in the Scientific and Technical Sphere, the contract No. 5242GC1/101612, dated November 07, 2024.

Funding

Modeling of effective properties of compacted reaction media under conditions of microwave heating was sup-

ported by the grant of the Russian Science Foundation № 23-19-00363, <https://rscf.ru/project/23-19-00363/>

Conflict of interest

The authors declare that they have no conflict of interest.

References

- [1] J.R. Chamorro, T.M. McQueen. *Accounts Chem. Res.*, **51** (11), 2918 (2018). DOI: 10.1021/acs.accounts.8b00382
- [2] A.V. Samokhin, N.V. Alekseev, S.A. Kornev, M.A. Sinaiskii, Yu.V. Blagoveschenskiy, A.V. Kolesnikov. *Plasma Chem. Plasma Process*, **33**, 605 (2013). DOI: 10.1007/s11090-013-9445-9
- [3] A.C.H. Barreto, V.R. Santiago, R.M. Freire, S.E. Mazzetto, J.M. Sasaki, I.F. Vasconcelos, J.C. Denardin, G. Mele, L. Carbone, P.B.A. Fachine. *J. Mater. Eng. Performance*, **22**, 2073 (2013). DOI: 10.1007/s11665-013-0480-8
- [4] H.J. Kitchen, S.R. Vallance, J.L. Kennedy, N. Tapia-Ruiz, L. Carassiti, A. Harrison, A.G. Whittaker, T.D. Drysdale, S.W. Kingman, D.H. Gregory. *Chem. Rev.*, **114** (2), 1170 (2014). DOI: 10.1021/cr4002353
- [5] Y. Makino. *ISIJ Int.*, **47** (4), 539 (2007). DOI: 10.2355/isijinternational.47.539
- [6] K.J. Rao, B. Vaidyanathan, M. Ganguli, P.A. Ramakrishnan. *Chem. Mater.*, **11** (4), 882 (1999). DOI: 10.1021/cm9803859
- [7] C.O. Kappe. *Amer. Labor*, **33**, 13 (2001). DOI: 10.1002/chin.200222256
- [8] S. Dabrowska, T. Chudoba, J. Wojnarowicz, W. Łojkowski. *Crystals*, **8** (10), 379 (2018). DOI: 10.3390/cryst8100379
- [9] C. Leonelli, W. Łojkowski. *Chem. Today*, **25** (3), 34 (2007).
- [10] C. Leonelli, S. Komarneni. *Inorganics*, **3**, 388 (2015). DOI: 10.3390/inorganics3040388
- [11] M.A. Imam, D. Lewis, R.W. Bruce, A.W. Fliflet, L.K. Kurihara. *Mater. Sci. Forum*, **426–432** (5), 4111 (2003). DOI: 10.4028/www.scientific.net/MSF.426-432.4111
- [12] K. Essaki, E.J. Rees, G.T. Burstein. *J. Amer. Ceram. Soc.*, **93** (3), 692 (2009). DOI: 10.1111/j.1551-2916.2009.03462.x
- [13] A.V. Samokhin, N.V. Alekseev, M.A. Sinayskiy, A.G. Astashov, A.V. Vodopyanov, A.A. Sorokin, S.V. Sintsov. *Intern. J. Refractory Metals and Hard Materials*, **100**, 105618 (2021). DOI: 10.1016/j.ijrmhm.2021.105618
- [14] A. Karimzadeh, B. Arman, H. Masoud, S. Email, M.Sh. Bafghi, K. Yanagisawa. *Int. J. Min. Metall. Mater.*, **24** (2), 202 (2017). DOI: 10.1007/s12613-017-1396-3
- [15] Yu. Bykov, A. Ereemeev, M. Glyavin, V. Kholoptsev, A. Luchinin, I. Plotnikov. *IEEE Transactions Plasma Sci.*, **32** (1), 67 (2004). DOI: 10.1109/TPS.2004.823904
- [16] Yu.V. Bykov, A.G. Ereemeev, M.Yu. Glyavin, G.G. Denisov, G.I. Kalynova, E.A. Kopelovich, A.G. Luchinin, I.V. Plotnikov, M.D. Proyavin, M.M. Troitskiy, V.V. Kholoptsev. *Radiophys Quantum El.*, **61**, 752 (2019). DOI: 10.1007/s11141-019-09933-6
- [17] A.G. Litvak, G.G. Denisov, M.Y. Glyavin. *IEEE J. Microwaves*, **1** (1), 260 (2021). DOI: 10.1109/JMW.2020.3030917
- [18] D.A.G. Bruggeman. *Ann. Phys.*, **416**, 636 (1935). DOI: 10.1002/andp.19354160705
- [19] H. Liu, L. Guo, L. Zou, M. Cao, J. Zhou, S. Ouyang. *Mater. Sci. Eng. B*, **113** (2), 161 (2004). DOI: 10.1016/j.mseb.2004.07.082
- [20] S.V. Egorov, A.G. Ereemeev, V.V. Kholoptsev, I.V. Plotnikov, K.I. Rybakov, A.A. Sorokin, S.S. Balabanov, E.Ye. Rostokina. *Materialia*, **24**, 101513 (2022). DOI: 10.1016/j.mtla.2022.101513
- [21] P. Schupp. *Z. Physik*, **75**, 84 (1932). DOI: 10.1007/BF01340516
- [22] G.V. Samsonov *Physiko-khimicheskie svoistva okislov* (*Metallurgiya*, M., 1978) (in Russian).
- [23] Z. Weng, C. Wu, Z. Xiong, Y. Feng, H. Amini Rastabi, C. Song, H. Xue. *J. Eur. Ceram. Soc.*, **37**, 4667 (2017). DOI: 10.1016/j.jeurceramsoc.2017.06.039
- [24] R.S. Bever, R.L. Sproull. *Phys. Rev.*, **83**, 801 (1951). DOI: 10.1103/PhysRev.83.801
- [25] K. Kashimura, H. Sugawara, M. Hayashi, T. Mitani, N. Shinohara. *AIP Adv.*, **6**, 065001 (2016). DOI: 10.1063/1.4953325
- [26] L. Momenzadeh, B. Moghtaderi, O. Buzzi, X. Liu, S.W. Sloan, G.E. Murch. *Comp. Mater. Sci.*, **141**, 170 (2018). DOI: 10.1016/j.commatsci.2017.09.033
- [27] M. Tachibana, C. Bourges, T. Mori. *Appl. Phys. Express*, **15**, 121003 (2022). DOI: 10.35848/1882-0786/ac9d21
- [28] I.S. Grigor'ev, E.Z. Meilikhov. *Fizicheskie velichiny, spravochnik* (*Energoatomizdat*, M., 1991) (in Russian).

Translated by M. Shevelev